# Magnetocaloric Effect in AlFe$_2$B$_2$: Toward Magnetic Refrigerants from Earth-Abundant Elements

Xiaoyan Tan, Ping Chai, Corey M. Thompson,[†] and Michael Shatruk*

Department of Chemistry and Biochemistry, Florida State University, 95 Chieftan Way, Tallahassee, Florida 32306, United States

S Supporting Information

ABSTRACT: AlFe$_2$B$_2$ was prepared by two alternative synthetic routes, arc melting and synthesis from Ga flux. In the layered crystal structure, infinite chains of B atoms are connected by Fe atoms into two-dimensional [Fe$_2$B$_2$] slabs that alternate with layers of Al atoms. As expected from the theoretical analysis of electronic band structure, the compound exhibits itinerant ferromagnetism, with the ordering temperature of 307 K. The measurement of magnetocaloric effect (MCE) as a function of applied magnetic field reveals isothermal entropy changes of 4.1 J kg^{-1} K^{-1} at 2 T and 7.7 J kg^{-1} K^{-1} at 5 T. These are the largest values observed near room temperature for any metal boride and for any magnetic material of the vast 122 family of layered structures. Importantly, AlFe$_2$B$_2$ represents a rare case of a lightweight material prepared from earth-abundant, benign reactants which exhibits a substantial MCE while not containing any rare-earth elements.
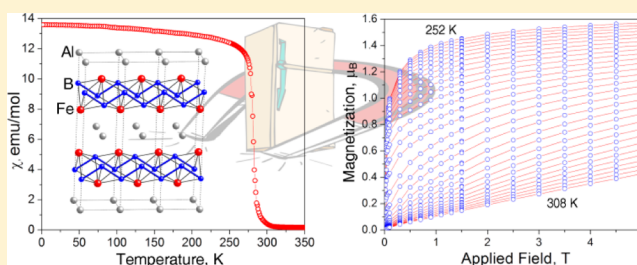
1. INTRODUCTION

Magnetic refrigeration is a promising, environmentally friendly technology that provides appealing energy-conversion efficiencies.[1] It relies on the magnetocaloric effect (MCE) discovered by Warburg in 1881[2] and defined as a reversible change in the magnetic component of total entropy (and temperature) of a material upon application or removal of magnetic field. Since pioneering works of Giauque and Debye,[3] this effect has been used to achieve sub-Kelvin temperatures by adiabatic demagnetization of paramagnetic salts.[4] The discovery of a giant MCE in Gd$_5$Si$_2$Ge$_2$ near room temperature[5] has led to an explosion of research activities in this area, in the effort to implement magnetic refrigeration as a viable replacement for the current gas compression−expansion technology.[1,6] Nevertheless, a practically applicable magnetocaloric material that could provide sustainable operation in the magnetic field created by strong permanent magnets (<2 T) is yet to be found.

At present, 15 years after the initial report of giant MCE in Gd$_5$Si$_2$Ge$_2$,[5] only a handful of compounds have matched or approached its performance. Most prominent materials with giant MCE around room temperature include MnFe(P$_{1-x}$As$_x$),[7] FeRh,[8] LaFeSi$_{13}$,[9] Heusler alloys,[10] and their substituted variants. Importantly, all of them are magnetically soft, resulting in minimal hysteresis losses, which would be detrimental to the cooling effect. We also note that all these materials exhibit itinerant magnetism that emerges from spin polarization of the electronic band structure at the Fermi level.

Metal borides are often thought of as magnetically hard materials, obviously due to the famous Nd$_2$Fe$_{14}$B—the strongest permanent-magnet material known.[11] This magnetic hardness, however, stems from the strong anisotropy of the rare-earth sublattice. Indeed, most transition metal borides are soft magnets, and imparting magnetic hardness to rare-earth free borides represents another fundamental research challenge.[12]

Interested in the possibility to observe a large MCE in systems significantly different from the ones explored heretofore, we thus turned our attention to transition metal borides. The simplest borides, such as FeB or MnB, are not appropriate for this purpose, because of very high ferromagnetic ordering temperatures (598 K[13] and 562 K,[14] respectively). It is desirable to "dilute" the magnetic sublattice of these materials in order to bring the magnetic phase transition to room temperature. In 1969, Jeitschko reported the structure of AlFe$_2$B$_2$ and suggested that this material might be ferromagnetic.[15] As we will show below, this prediction is also supported by band structure calculations. Indeed, a recent report demonstrated ferromagnetic ordering in AlFe$_2$B$_2$ around 300 K, but did not elucidate its magnetization and magnetocaloric properties.[16] Furthermore, the magnetic measurements were performed on a material contaminated with notable impurities, which precludes an accurate evaluation of its MCE.

This lightweight material appears especially appealing to us, given its being composed of earth-abundant, benign reactants. Herein, we report the synthesis of phase-pure AlFe$_2$B$_2$ by two different synthetic methods and a detailed investigation of its magnetic behavior and magnetocaloric properties. We demonstrate that this compound exhibits a significant MCE, thus identifying another class of solids for the exploration of novel magnetic refrigerants.

2. MATERIALS AND METHODS

Starting Materials. Aluminum powder (99.95%) and gallium pellets (99.99%) were bought from Alfa Aesar. Boron powder (95–97%) was obtained from Strem Chemicals. All these materials were used as received. Iron powder (Alfa Aesar, 98%) was further purified by heating under a flow of H_2 gas at 773 K for 5 h. During sample preparation, all operations were carried out in an argon-filled glovebox (concentration of $O_2 < 1$ ppm).

Synthesis. *Method A: Arc-Melting (Sample 1a).* The starting materials were mixed in the Al:Fe:B = 3:2:2 ratio (total mass = 0.35 g) and pressed into a 10 mm i.d. pellet. An excess amount of Al is crucial for obtaining the desired phase and minimizing the content of byproducts. The pellet was arc-melted under argon. To improve homogeneity of the product, the obtained ingot was sealed under vacuum ($<10^{-2}$ mbar) in a 10 mm i.d. silica tube and annealed at 1173 K for 7 days. Powder X-ray diffraction analysis indicated that the samples contained $AlFe_2B_2$ as the major phase and an impurity of $Al_{13}Fe_4$. The byproduct was removed by soaking the sample in dilute HCl (1:1 v/v) for 10 min. $AlFe_2B_2$ also reacts with dilute HCl but at a much slower rate. The phase purity of the product after acid treatment was confirmed by powder X-ray diffraction.

Method B: Synthesis from Ga Flux (Sample 1b). The starting materials were mixed in the Al:Fe:B:Ga = 1.5:1.8:2:10 ratio (total mass = 2 g) and loaded into a 10 mm i.d. alumina crucible. The crucible was placed in a 13 mm i.d. silica tube and sealed under vacuum ($<10^{-2}$ mbar). The mixture was annealed at 1173 K for 7 days. The Ga flux was removed by centrifugation at 600 °C. To remove the remaining traces of Ga, the product was soaked in a 1.5 M solution of I_2 in N,N'-dimethylformamide (DMF). Powder X-ray diffraction confirmed the phase purity of the sample obtained.

X-ray Diffraction. Room temperature powder X-ray diffraction (PXRD) was carried out on a PANalytical X'Pert Pro diffractometer with an X'Celerator detector using Cu Kα radiation ($\lambda = 1.54187$ Å). The FullProf software package[17] was used for profile fitting and unit cell refinement.

Physical Measurements. Magnetic measurements were performed on polycrystalline samples with a Quantum Design SQUID magnetometer MPMS-XL. DC magnetic susceptibility measurements were carried out in an applied field of 1 mT in the 1.8–350 K temperature range. Magnetization and hysteresis were measured at 1.8 K with the magnetic field varying between −7 and 7 T. For MCE calculations, isothermal dependences of magnetization were collected in the temperature range of 252–232 K with a step of 2 K. The magnetic field was increased in 0.02 T, 0.2 T, and 0.5 T increments for the range of 0–0.1 T, 0.1–1.5 T, and 1.5–5 T, respectively. The heat capacity was measured with a Quantum Design Physical Property Measurement System in the temperature range of 1.8–350 K in zero applied field.

Quantum-Chemical Calculations. Density-functional theory (DFT) band structure calculations were performed with a full potential all-electron local orbital code FPLO (version fplo7.00-28) within the local spin density approximation (LSDA).[18] The Perdew–Wang parametrization of the exchange-correlation potentials was employed.[19] The scalar-relativistic Dirac equation was solved self-consistently. The tetrahedron method was used for the Brillouin-zone integration.[20] The structural parameters (unit cell dimensions and atomic coordinates) were taken from the reported room-temperature crystal structure of $AlFe_2B_2$.[15] The nonpolarized and spin-polarized density of states (DOS) were calculated after convergence of the total energy on a dense k-mesh with 32 × 32 × 32 points. The self-consistent criterion for the total energy conversion was equal to 10^{-8} Ha ($\sim 2.72 \times 10^{-7}$ eV).

3. RESULTS AND DISCUSSION

Synthesis. $AlFe_2B_2$ (**1a**) was obtained as a major phase after arc-melting a compact pellet of Al, Fe, and B premixed in the 3:2:2 ratio. A significant amount of $Al_{13}Fe_4$ is present as a byproduct (Figure 1a), as was also observed in the earlier
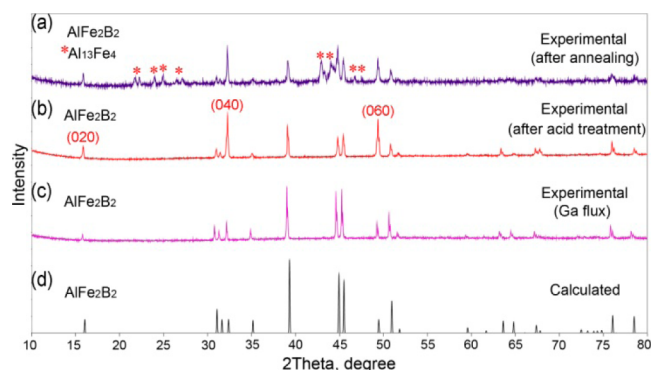

Figure 1. X-ray powder diffraction patterns of $AlFe_2B_2$ obtained by arc-melting a mixture of elements (a), after treating the products of arc-melting with dilute HCl for ~10 min (b; sample **1a**; the enhanced (0*k*0) reflections are indicated), and by the reaction between elements in Ga flux (c; sample **1b**). A pattern calculated on the basis of the crystal structure of $AlFe_2B_2$[15] is shown for comparison (d).

report.[16] Decreasing the content of Al in the reactant mixture to the stoichiometric amount results in the formation of FeB byproduct, which is difficult to separate from $AlFe_2B_2$. We determined that the 3:2:2 ratio of Al:Fe:B prevents the formation of FeB while still keeping the content of $Al_{13}Fe_4$ relatively low. The latter is easily removed by treating the mixture with a dilute HCl solution for ~10 min (Figure 1b). $AlFe_2B_2$ also reacts with dilute HCl but at a much slower rate. The intensity redistribution observed in the PXRD pattern of **1a** as compared to the theoretically calculated one (Figure 1d) stems from preferred orientation of crystallites evidenced by the enhancement of (0*k*0) lines in the experimental pattern of **1a**.

In an attempt to obtain $AlFe_2B_2$ by an alternative synthetic technique, we explored the reaction between the constituent elements in Ga flux. It was proposed that Ga could serve as promising medium for the preparation of borides because it dissolves elemental boron without forming any binary Ga–B compounds.[21] (We have recently demonstrated the effectiveness of a similar approach to the preparation of arsenides from Bi flux.[22]) Indeed, a reaction in Ga flux, with subsequent removal of Ga by centrifugation and I_2/DMF treatment, led to a phase-pure sample of $AlFe_2B_2$ (**1b**, Figure 1c). The experimental PXRD pattern is in good agreement with the one calculated from the crystal structure of $AlFe_2B_2$.[15] Sample **1b** was obtained as fine powder as compared to sample **1a** that was obtained as an ingot and ground manually. Thus, the preferred orientation observed in the PXRD pattern of **1a** most probably was introduced by grinding the sample after arc-melting.

Crystal Structure. $AlFe_2B_2$ crystallizes in an orthorhombic lattice. The unit cell parameters refined from the PXRD data (Figure S1 in Supporting Information [SI]) agree well with those reported independently by Jeitschko[15] and Kuz'ma and Chaban[23] (Table 1) who briefly discussed its crystal structure. We provide here a more detailed view of this structure, focusing

Table 1. Unit Cell Parameters and Volume of $AlFe_2B_2$

sample	a, Å	b, Å	c, Å	V, Å^3
$AlFe_2B_2$ (**1a**)	2.9283(3)	11.0334(4)	2.8682(3)	92.669(3)
$AlFe_2B_2$ (**1b**)	2.9311(2)	11.0376(3)	2.8783(2)	93.119(2)
$AlFe_2B_2$[15]	2.923	11.034	2.870	92.58
$AlFe_2B_2$[23]	2.923	11.046	2.875	92.83

especially on its layered buildup. The layered structure of $AlFe_2B_2$ is reminiscent of well-known ternary structure types of the same stoichiometry, $ThCr_2Si_2$ and $CaAl_2Si_2$, in which slabs of $[Cr_2Si_2]$ and $[Al_2Si_2]$, respectively, alternate with the layers of electropositive metal atoms. The buildup of $AlFe_2B_2$, however, is significantly different in that the nonmetal B atoms appear not on the outside but in the middle of the $[Fe_2B_2]$ slab, and the slabs do not exhibit tetragonal symmetry. The $[Fe_2B_2]$ layer can be viewed as built of infinite zigzag chains of B atoms that run along the a axis, with each B atom forming two B−B bonds at 1.74 Å. When viewed along the c axis, these chains appear as a corrugated layer (Figure 2a). Fe
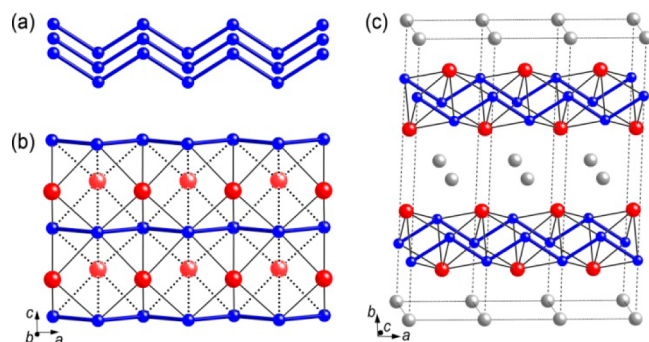

Figure 2. Crystal structure of $AlFe_2B_2$: zigzag chains of B atoms (a) are connected into a two-dimensional slab by Fe atoms (b), and the slabs are separated by layers of Al atoms (c). Color scheme: Al = gray, Fe = red, B = blue.

atoms are positioned between the chains, above and below this layer, in such a way that they "stitch" the boron chains into the two-dimensional slab. Each Fe atom forms six Fe−B bonds with B atoms from two neighbor chains (Figure 2b). Thus, each individual Fe layer has an approximate tetragonal symmetry, but the top and bottom Fe layers in the same $[Fe_2B_2]$ slab are shifted with respect to each other along the a axis to satisfy the bonding requirements of the boron zigzag chains. The $[Fe_2B_2]$ slabs are alternating along the b axis with layers of Al atoms (Figure 2c). Each Al atom is surrounded by a distorted cube of Fe atoms and two axial B atoms, with Al−Fe and Al−B interatomic distances of 2.61 Å and 2.29 Å, respectively.

Electronic Structure. The electronic band structure of $AlFe_2B_2$ was calculated at the density functional level of theory using the FPLO code.[18] The calculated nonpolarized DOS exhibits a strong maximum at the Fermi level, mainly due to the contribution from Fe 3d states (Figure 3). The Stoner criterion
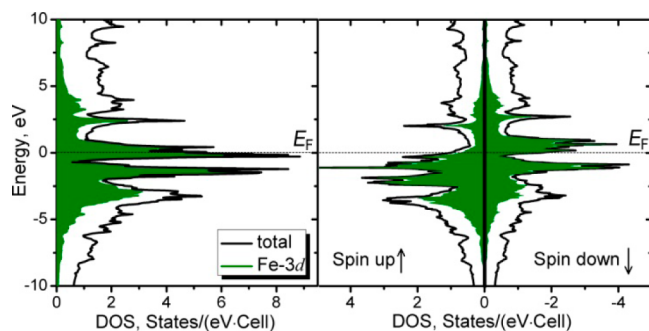

Figure 3. Nonpolarized (left) and spin-polarized (right) electronic density of states for $AlFe_2B_2$. The contribution from the Fe 3d orbitals is shown in green. The Fermi level is indicated with a dotted line.

for ferromagnetism is formulated as $J \cdot n(E_F) > 1$,[24] where J is a measure of the magnetic exchange interaction between 3d metal ions and $n(E_F)$ is the DOS at the Fermi level. The value of J can be taken approximately equal to the one reported for elemental Fe, 0.46 eV,[25] resulting in $J \cdot n(E_F) \approx 1.11$ per Fe atom. Thus, the Stoner criterion is satisfied, and one could expect $AlFe_2B_2$ to exhibit ferromagnetic ordering. Consequently, we performed spin-polarized band structure calculations that led to the expected magnetic moment of 1.25 μ_B per Fe atom.

Magnetic Properties. The magnetic measurements were performed on polycrystalline samples of $AlFe_2B_2$ obtained by arc-melting (**1a**) or by annealing in Ga flux (**1b**). For both samples, a spontaneous magnetization is observed, indicating ferromagnetic phase transition at 282(1) K and 307(1) K, respectively (Figure 4). The accurate values of T_C were
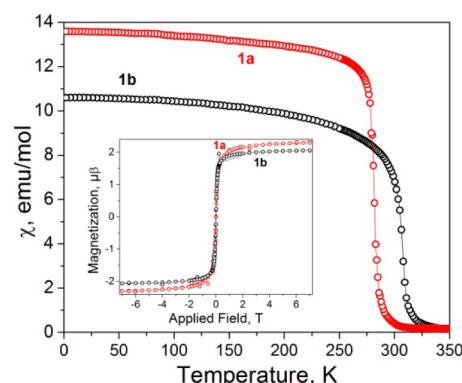

Figure 4. Temperature dependence of magnetic susceptibility for $AlFe_2B_2$ obtained by arc-melting (**1a**) and by synthesis in Ga flux (**1b**). Inset: field-dependent magnetization measured at 1.8 K.

established from Arrott plots as corresponding to the isotherm at which the change in the curvature of the M^2 vs H/M dependence is observed (Figure S2 in SI). The field-dependent magnetization measurements performed at 1.8 K revealed negligible coercivity, indicating that $AlFe_2B_2$ is a soft ferromagnet (Figure 4, inset). The saturation magnetization values measured for **1a** and **1b** were 1.15 μ_B and 1.03 μ_B per Fe atom, respectively, which are in good agreement with the theoretically predicted value of 1.25 μ_B per Fe atom. The slight difference in the ordering temperature and saturation magnetization of **1a** and **1b**, most probably stems from the different postsynthesis treatment of the samples, as mentioned in the discussion of the PXRD patterns.

Magnetocaloric Effect. The ferromagnetic ordering near room temperature and magnetic softness of $AlFe_2B_2$ incited us to evaluate its magnetocaloric properties. The magnetic entropy change (ΔS_m) was calculated from magnetization isotherms recorded in the range of 252−308 K for **1a** and 288−332 K for **1b**. The integral in the Maxwell equation,

$$\Delta S_m(T, \Delta H) = \int_0^{H_{max}} \left(\frac{\partial M}{\partial T} \right)_H dH \tag{1}$$

was approximated by a sum,

$$\Delta S_m(T_i, \Delta H) = \sum_0^{H_{max}} \frac{M_i - M_{i-1}}{T_i - T_{i-1}} \Delta H \tag{2}$$

where the change in the magnetic entropy for each temperature increment, $T_{i+1} - T_i$, was calculated by summing the incremental changes in the magnetization, $M_{i+1} - M_i$, produced by the stepwise (ΔH) increase in the magnetic field from 0 to H_{max}. The maximum entropy change is observed around T_C, with the calculated values of $-\Delta S_m = 4.4(3)$ and $7.3(5)$ J kg^{-1} K^{-1} for **1a** and $4.1(3)$ and $7.7(6)$ J kg^{-1} K^{-1} for **1b** at $H_{max} = 2$ and 5 T, respectively.[26] Using the calculated values of ΔS_m, one can also estimate the relative cooling power, RCP, as the product of the maximum value of $-\Delta S_m$ and the full-width at half-maximum (fwhm) of the ΔS_m peak (Figure 5b). The RCP values thus obtained are listed in Table 2.
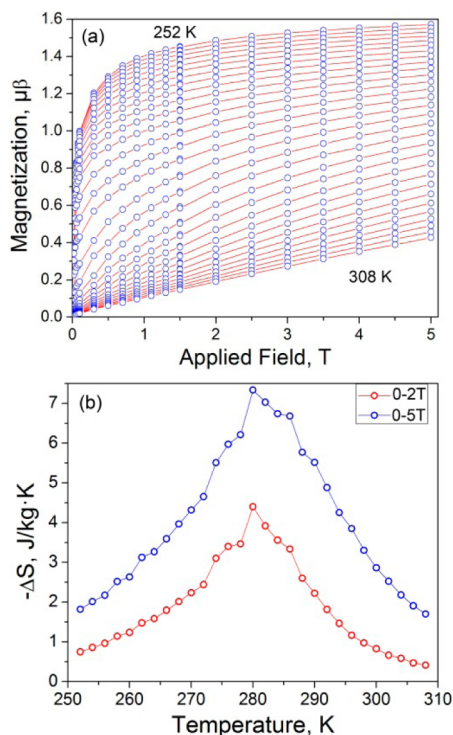

Figure 5. (a) Magnetization isotherms for $AlFe_2B_2$ obtained by arc-melting (sample **1a**). (b) The magnetic entropy changes calculated for the magnetic field change of 2 and 5 T. (See Figure S3 in SI for magnetocaloric data of sample **1b**.)

Table 2. Magnetic and Magnetocaloric Characteristics of Samples 1a and 1b in Comparison to Benchmark Materials

compound	T_C, K	$-\Delta S_m$, J kg^{-1} K^{-1} 2 T/5 T	ΔT_{ad}, K 2 T/5 T	RCP, J kg^{-1} 2 T/5 T
$AlFe_2B_2$				
1a	282	4.4/7.3	1.8/3.0	88/210
1b	307	4.1/7.7		53/162
$Gd_5Si_2Ge_2$[5]	276	14/19	7.3/15	126/460
$MnFeP_{0.45}As_{0.55}$[7]	300	14.5/18	–	174/414
$PrMn_2Ge_{0.8}Si_{1.2}$[27a]	303	1.0/2.2	–	–

The adiabatic temperature change (ΔT_{ad}) can be calculated as an isoentropic difference between two $S(H,T)$ curves measured at constant magnetic fields. The $S(0,T)$ curve was established from zero-field heat capacity measurements on sample **1a** as $S = \int_0^T (C_p/T) dT$ (Figure S4 in SI). Since $\Delta S_m(H,T)$ was determined from magnetization measurements (Figure 5), the $S(H = 2\ T)$ and $S(H = 5\ T)$ curves were obtained by subtracting the $\Delta S_m(H,T)$ values from $S(0,T)$

values measured at the same temperature (Figure S5 in SI). Once the total isofield entropy curves were established as a function of temperature, the ΔT_{ad} was found as the isoentropic difference between $S(H = H_{max})$ and $S(H = 0\ T)$, resulting in $\Delta T_{ad} = 1.8$ and 3.0 K at $H_{max} = 2$ and 5 T, respectively (Figure S6 in SI).

4. CONCLUSIONS

The magnetocaloric effect (MCE) in $AlFe_2B_2$, characterized by the values of ΔS_m and ΔT_{ad}, is lower than the MCE tabulated for such benchmarks as $Gd_5Si_2Ge_2$[5] and $MnFeP_{0.45}As_{0.55}$[7] (Table 2). Nevertheless, it is essential to point out that (1) $AlFe_2B_2$ is composed of light, earth-abundant elements, and (2) the MCE of $AlFe_2B_2$ exceeds the values observed around room temperature for any boride or any 1-2-2 type intermetallics heretofore.[27] As noted above, transition-metal borides remain essentially unexplored vis-à-vis their magnetocaloric properties. The results reported herein clearly demonstrate the potential of this class of materials to exhibit large MCE. In this vein, we have searched for other borides whose band structure, similar to $AlFe_2B_2$, would exhibit a high DOS peak at the Fermi level, which is a prerequisite for itinerant ferromagnetism. Our preliminary calculations indicate that compounds RFe_2B_2 (R = Y, Gd) also should exhibit ferromagnetic ordering. There exists one report of such borides in the literature,[28] but these materials were not obtained in phase-pure form and their magnetic properties were not investigated. We are currently exploring various synthetic approaches toward phase-pure samples of these materials, and if these efforts prove successful, the magnetic and magnetocaloric properties of RFe_2B_2 will be reported in due course.

■ ASSOCIATED CONTENT

Ⓢ Supporting Information
Full-pattern profile fitting of PXRD data, heat capacity and additional magnetic plots. This material is available free of charge via the Internet at http://pubs.acs.org.

■ AUTHOR INFORMATION

Corresponding Author
shatruk@chem.fsu.edu
Present Address
†Department of Chemistry, McMaster University, 1280 Main Street West, Hamilton, ON, Canada L8S 4M1.
Notes
The authors declare no competing financial interest.

■ ACKNOWLEDGMENTS

■ REFERENCES

(1) Franco, V.; Blazquez, J. S.; Ingale, B.; Conde, A. *Annu. Rev. Mater. Res.* **2012**, *42*, 305−342.
(2) Warburg, E. *Ann. Phys.* **1881**, *13*, 141−164.
(3) (a) Giauque, W. F. *J. Am. Chem. Soc.* **1927**, *49*, 1864−1870. (b) Debye, P. *Ann. Phys.* **1926**, *81*, 1154−1160.
(4) (a) Giauque, W. F.; MacDougall, D. P. *J. Am. Chem. Soc.* **1935**, *57*, 1175−1185. (b) de Haas, W. J.; Wiersma, E. C.; Kramers, H. A. *Naturwissenschaften* **1933**, *21*, 467.

(5) Pecharsky, V. K.; Gschneidner, K. A., Jr. *Phys. Rev. Lett.* **1997**, *78*, 4494−4497.

(6) (a) Gschneidner, K. A., Jr.; Pecharsky, V. K.; Tsokol, A. O. *Rep. Prog. Phys.* **2005**, *68*, 1479−1539. (b) Brück, E. *Handb. Magn. Mater.* **2007**, *17*, 235−291. (c) Shen, B. G.; Sun, J. R.; Hu, F. X.; Zhang, H. W.; Cheng, Z. H. *Adv. Mater.* **2009**, *21*, 4545−4564. (d) Morrison, K.; Lyubina, J.; Moore, J. D.; Sandeman, K. G.; Gutfleisch, O.; Cohen, L. F.; Caplin, A. D. *Philos. Mag.* **2012**, *92*, 292−303.

(7) Tegus, O.; Brück, E.; Buschow, K. H. J.; de Boer, F. R. *Nature* **2002**, *415*, 150−152.

(8) Manekar, M.; Roy, S. B. *J. Phys. D: Appl. Phys.* **2008**, *41*, 192004.

(9) (a) Gutfleisch, O.; Yan, A.; Müller, K. H. *J. Appl. Phys.* **2005**, *97*, 10M305. (b) Han, M. K.; Miller, G. J. *Inorg. Chem.* **2008**, *47*, 515−528.

(10) (a) Krenke, T.; Duman, E.; Acet, M.; Wassermann, E. F.; Moya, X.; Manosa, L.; Planes, A. *Nat. Mater.* **2005**, *4*, 450−454. (b) Hu, F. X.; Shen, B. G.; Sun, J. R.; Wu, G. H. *Phys. Rev. B* **2001**, *64*.

(11) Gutfleisch, O.; Willard, M. A.; Brück, E.; Chen, C. H.; Sankar, S. G.; Liu, J. P. *Adv. Mater.* **2011**, *23*, 821−842.

(12) (a) Fokwa, B. P. T.; Lueken, H.; Dronskowski, R. *Eur. J. Inorg. Chem.* **2011**, 3926−3930. (b) Brgoch, J.; Goerens, C.; Fokwa, B. P. T.; Miller, G. J. *J. Am. Chem. Soc.* **2011**, *133*, 6832−6840.

(13) Chien, C. L.; Unruh, K. M. *Phys. Rev. B* **1984**, *29*, 207−211.

(14) Miryasov, N. Z.; Parsanov, A. P. *Izv. Akad. Nauk SSSR Ser. Fiz.* **1959**, *23*, 285−8.

(15) Jeitschko, W. *Acta Crystallogr., Sect. B* **1969**, *25*, 163−165.

(16) El Massalami, M.; Oliveira, D. d.; Takeya, H. *J. Magn. Magn. Mater.* **2011**, *323*, 2133−2136.

(17) Rodríguez-Carvajal, J. *Physica B* **1993**, *192*, 55−69.

(18) (a) Koepernik, K.; Eschrig, H. *Phys. Rev. B* **1999**, *59*, 1743−1757. (b) Opahle, I.; Koepernik, K.; Eschrig, H. *Phys. Rev. B* **1999**, *60*, 14035−14041.

(19) Perdew, J. P.; Wang, Y. *Phys. Rev. B* **1992**, *45*, 13244−13249.

(20) Blochl, P. E.; Jepsen, O.; Andersen, O. K. *Phys. Rev. B* **1994**, *49*, 16223−16233.

(21) (a) Kanatzidis, M. G.; Pöttgen, R.; Jeitschko, W. *Angew. Chem., Int. Ed.* **2005**, *44*, 6996−7023. (b) Salvador, J. R.; Bilc, D.; Mahanti, S. D.; Kanatzidis, M. G. *Angew. Chem., Int. Ed.* **2002**, *41*, 844−846.

(22) Thompson, C. M.; Kovnir, K.; Eveland, S.; Herring, M. J.; Shatruk, M. *Chem. Commun.* **2011**, *47*, 5563−5565.

(23) Kuz'ma, Y.; Chaban, N. F. *Neorg. Mater.* **1969**, *5*, 384−385.

(24) Stoner, E. C. *Proc. Royal Soc. A* **1938**, *165*, 372−414.

(25) Janak, J. F. *Phys. Rev. B* **1977**, *16*, 255−262.

(26) The standard deviations in the MCE values were optimistically estimated at 7.5% following the error analysis provided in Pecharsky, V. K.; Gschneidner, K. A., Jr. *J. Appl. Phys.* **1999**, *86*, 565−575.

(27) (a) Wang, J. L.; Campbell, S. J.; Zeng, R.; Poh, C. K.; Dou, S. X.; Kennedy, S. J. *J. Appl. Phys.* **2009**, *105*. (b) Chen, Y. Q.; Luo, J.; Liang, J. K.; Li, J. B.; Rao, G. H. *J. Alloys Compd.* **2010**, *489*, 13−19. (c) Emre, B.; Dincer, I.; Elerman, Y. *J. Magn. Magn. Mater.* **2010**, *322*, 448−453.

(28) Stepanchikova, G. F.; Kuz'ma, Y. B.; Chernyak, B. I. *Dopov. Akad. Nauk USSR A* **1978**, 950−952.

9557

dx.doi.org/10.1021/ja404107p | *J. Am. Chem. Soc.* 2013, 135, 9553−9557